Coventry University and
The University of Wisconsin Milwaukee Centre for By-products Utilization,
Second International Conference on Sustainable Construction Materials and Technologies
June 28 - June 30, 2010, Università Politecnica delle Marche, Ancona, Italy.
Main Proceedings ed. J Zachar, P Claisse, T R Naik, E Ganjian. ISBN 978-1-4507-1490-7
http://www.claisse.info/Proceedings.htm

Time-Variant Capacity and Reliability of GFRP-Reinforced Bridge Decks

Young Hoon Kim[1], Paolo Gardoni[2], and David Trejo[3]

1) Post Doctoral Research Associate, Civil and Construction Engineering, Oregon State University, 220 Owen Hall, Corvallis, OR 97331. E-mail: <yhkim05@oregonstate.edu>
2) Associate Professor, Texas A&M University, TAMU, College Station, TX 77843. E-mail: <pgardoni@civil.tamu.edu>
3) Professor and Construction Education Foundation Endowed Chair, Civil and Construction Engineering, Oregon State University, 220 Owen Hall, Corvallis, OR 97331. E-mail: <david.trejo@oregonstate.edu>

ABSTRACT

Glass-fiber reinforced polymer (GFRP) reinforcement is being used in bridge decks as a replacement for steel reinforcement. It is thought that since the GFRP reinforcement does not corrode, it can be a more sustainable material for reinforced concrete structures. Limited research has been performed to quantify the time-variant capacity of GFRP reinforcement embedded in concrete and thus the applicability of the environmental factor found in American Concrete Institute (ACI) 440 is questionable. A Bayesian approach was used to develop time-variant probabilistic capacity models based on data of the capacity of GFRP reinforcement embedded in concrete for a period of 7 years. These models are used herein to assess the time-variant structural reliability of a bridge deck. The results on the ability of GFRP-reinforced bridges to withstand future loads can be used to optimize the allocation of resources for maintenance, repair, and rehabilitation for the design and construction of sustainable bridge systems.

INTRODUCTION

Glass fiber-reinforced polymer (GFRP) reinforcement has emerged as a potential alternative to conventional steel reinforcing bars for concrete structures. GFRP reinforcing bars have been identified as having non-corrosive characteristics, high tensile strength, and high strength to weight ratios. Considering the significant rehabilitation costs associated with the deterioration of existing bridges, mostly as a result of steel corrosion, the potential corrosion resistance of GFRP reinforcing bars could provide significant savings for structures containing reinforcement. The use of GFRP reinforcement has increased significantly in many infrastructure applications, including bridge decks, pavements, walls, and other systems. However, there is still a reluctance to use GFRP reinforcing bars. This reluctance results mostly from the lack of long-term performance data on GFRP reinforcing bars embedded in concrete.

Although GFRP reinforcing bars do not exhibit “classical” corrosion, many publications have reported that there is significant reduction in the tensile capacity of GFRP reinforcement when exposed to various solutions (Katsuki and Uomoto 1995; Tannous and Saadatmanesh 1999). Some literature is available on the reduction in the tensile capacity of GFRP reinforcement embedded in concrete, but these data are limited and based on short-term exposure periods (Almusallam et al. 2002; Giernacky et al. 2002; Mukherjee and Arwikar 2005). Because GFRP reinforcing bars are specifically designed for use in concrete and because the environmental exposure conditions inside concrete are significantly different than direct exposure to solutions, research is needed to better determine the influence of the concrete environment on the tensile capacity of GFRP reinforcement. The performance of GFRP reinforcement should be determined such that value is optimized while maintaining safety.

Significant research has been performed to assess the durability of GFRP reinforcing bars by measuring the change of the mechanical properties after exposure to various environments; mainly the tensile capacity and modulus of elasticity (MOE). Based on many accelerated exposure tests, models have been developed to predict the longer-term performance of these GFRP reinforcing bars. However, significant debate exists on the recommended models and the limits published in the design codes. This debate is a direct result of the lack of performance data from GFRP reinforcing bars embedded in concrete for longer periods under different exposure conditions. A "valid" prediction model that includes influencing parameters is needed.

Trejo et al. (2005) performed tests on the residual tensile strength of GFRP bars and reported that the tensile capacity could drop below the design capacity after just 7 years. These results were based on exposing the GFRP bars directly to water and alkaline solutions. However, it has been well established that concrete not continuously exposed to water does not have saturated pores and thus exposing the GFRP reinforcing bars to solution likely represents a worst case scenario of the GFRP performance.

Trejo et al. (2009, 2010) and Gardoni et al. (2010) developed probabilistic models to estimate the residual tensile capacity over time of GFRP bars. The models were developed using GFRP bars embedded in concrete for up to 7 years. The model was developed on the statistical assessment of the influence of the alkalinity of concrete, porosity of concrete, cover depth, and bar properties on the bar capacity. The model indicates that GFRP reinforcing bars with larger diameters exhibit lower rates of capacity loss.

Using the probabilistic model by Trejo et al. (2009, 2010) and Gardoni et al. (2010), this paper assesses the time-variant structural reliability of a typical bridge deck reinforced with GFRP bar. The GFRP reinforced decks containing two different sizes of the GFRP bars were used to evaluate the time-dependant degradation of the bridge deck as a function of bar size. The analysis can be used to predict the GFRP reinforced deck performance over time.

LITERATURE REVIEW

Many studies have been performed to assess the degree of degradation, the mechanism of degradation, and to characterize the parameters that impact the long-term characteristics of GFRP reinforcing bars. GFRP reinforcing bars are composed of aligned glass fibers surrounded by a polymer matrix, typically vinyl ester or polyester. When GFRP reinforcement has been used as an internal reinforcement in concrete, it has been widely reported that the tensile strength is reduced as a function of time (Almusallam et al. 2002; Giernacky et al. 2002; Mukherjee and Arwikar 2005). This is a result of "deterioration" of the glass fibers as a result of the presence of moisture and/or alkaline solution.

GFRP Reinforcing Bar Performance: Solution Exposure

A critical parameter influencing the deterioration rate of GFRP is the rate at which solution is transported into the GFRP reinforcing bar (Tannous and Saadatmanesh 1999). In addition to the condition of the environment surrounding the GFRP reinforcing bars, the mechanical properties could be affected by the imposed load on the bars, bar size, diffusion characteristics of the polymer matrix material, and temperature. Micelli and Nanni (2004) evaluated the reduction in tensile strength of GFRP bars. In this study the tensile strength of the GFRP specimens decreased by up to 59 and 70 percent after 21 and 42 days of immersion in alkaline solution, respectfully. Electron microscopy was used to identify the deterioration of the fiber, resin, and interfacial areas. This research demonstrated the importance of the resin in resisting the transport of elements or compounds towards the glass fibers and recommended the use of thermoplastic resins. Accelerated testing was performed by Micelli et al. (2001) and this research concluded that after exposure to alkaline solution the reduction in tensile strength as a function of time was dependent on resin type, specifically the absorption characteristics.

The changes in tensile strength, ultimate elongation, and MOE of GFRP reinforcing bars were also evaluated by Debaiky et al. (2006). The researchers used accelerated aging tests and found that the maximum reduction of tensile strength was 11 percent below the guaranteed ultimate tensile strength (GUTS) when exposed to a temperature of 60°C (140°F) and a sustained load of 29 percent of the GUTS. The ultimate strain was 43 percent higher than that recommended in the ACI 440.1R-03 (ACI 2003) design guidelines. No significant reduction in the elastic modulus was reported.

A wide range of results on the tensile capacity of GFRP bars have been reported. Although some literature reports limited changes in the residual tensile strength, a significant amount of research indicates that the tensile capacity of GFRP reinforcing bars decreases with time, some research showing significant reductions. However, this environment is significantly different than the concrete environment and the residual tensile capacity of GFRP bars immersed in solution could be significantly different than the residual capacity of GFRP bars embedded in concrete. The following section provides a review of the performance of GFRP bars embedded in concrete.

GFRP Reinforcing Bar Performance: Bars Embedded in Concrete

A number of studies have been performed to evaluate the influence of the concrete pore solution on the tensile capacity of GFRP reinforcement. Almusallam et al. (2002) reporteda reduction in tensile capacity of up to a 10.3% for unstressed GFRP bars and up to a 27.9% reduction in tensile capacity for stressed bars after only 120 days of embedment in concrete. Giernacky et al. (2002) reported s reduction in tensile capacity of almost 20% of the GFRP bars for beams subjected to a service load after only 180 days of embedment in concrete. Svecova et al. (2002) also reported significant reductions in GFRP tensile capacity; 36 to 53 percent reduction in tensile capacity for GFRP bars embedded in concrete beams immersed in a 140 ^{o}F (60 ^{o}C) water bath. Mukherjee and Arwikar (2005) reported GFRP reinforcing bars embedded in concrete beams and conditioned outdoors for 18 and 30 months exhibited residual strengths of approximately 61% of the unexposed GFRP bars (i.e., a 39 percent reduction). Robert et al. (2009) predicted losses up to 20% after 100 years. The author also reported that continuously immerged GFRP concrete specimens are field representative of exposure conditions when the concrete is continuously saturated

Although much research has reported significant loss in tensile capacity of GFRP bars, a field study conducted by Mufti et al. (2007a, b) concluded that the GFRP reinforcement is durable when embedded in concrete. Concrete cores reinforced with GFRP were removed from five structures located in North America. The GFRP bars were made with E-glass embedded in a vinyl ester resin and were embedment in concrete from 5 to 8 years. The structures were exposed to a wide range of environmental conditions. Scanning electron microscopy (SEM) and Energy dispersive X-ray analyses (EDX) were performed to detect possible degradation of the matrix and glass fibers. Fourier transform infrared spectroscopy (FTIR) was also used to estimate the changes in the glass transition temperature (*Tg*) of the resin. Based on these tests the authors reported no evidence of deterioration due to alkaline ingress and/or moisture absorption. The authors concluded that GFRP reinforcement is appropriate for use as reinforcement in concrete structures. However, no data on mechanical test results of the GFRP bars after embedment in the concrete environment were reported.

The literature clearly indicates that GFRP bars can exhibit degradation of capacity when embedded in solution and concrete. The rate and ultimate amount of this reduction is unknown, yet ACI Committee 440.1R (2007) and AASHTO LRFD Specifications (2008) require using an environmental reduction factor as a design parameter to consider the reduction in the tensile strength of GFRP in actual structures. This reduction factor, C_E, is dependent on the exposure conditions of the GFRP-reinforced concrete: for concrete not exposed to earth and weather the reduction factor is 0.8 and for concrete exposed to earth and weather the reduction factor is 0.7. The design tensile strength, σ_{ACI440}, of GFRP reinforcing bar considering these required reductions can then be determined as $\sigma_{\text{ACI440}} = C_E f_{fu}^*$, where f_{fu}^* is the GUTS of a FRP bar.

Further work is needed to assess and validate the time-variant capacity of GFRP bars when embedded in concrete. In addition, the influence of the reduced bar capacity on the structure capacity needs to be assessed. The following sections provide a methodology to predict the time-variant capacity of GFRP bars embedded in concrete and provide an example of the time-variant capacity of a typical GFRP-reinforced bridge deck designed using different diameters of GFRP reinforcing bars.

TIME-VARIANT CAPACITY OF GFRP BARS EMBEDDED IN CONCRETE

Trejo et al. (2009, 2010) and Gardoni et al. (2010) developed the following probabilistic model to predict the capacity of GFRP bars embedded in concrete over time, t:

$$\sigma_t\left(\mathbf{x}_b, \mathbf{\Theta}_b\right) = \left[\left(1 + s_0 \cdot e_0\right) - \lambda\left(\frac{D \cdot t}{R_0^2}\right)^{\alpha}\left(1 + s \cdot e\right)\right] \cdot \mu_{\sigma_0} \qquad (1)$$

where $\mathbf{x}_b = (D, R_0)$ is a vector of basic variables, D is the diffusion coefficient, R_o is the radius of the GFRP bar at $t = 0$, $s_0 \cdot e_0$ is an error term that captures the variability of the strength at $t = 0$ around its mean μ_{σ_0}, $s \cdot e$ is an error term that captures the variability in the reduction term $\lambda(D \cdot t / R_0^2)^{\alpha}$, e_0 and e are statistically independent normally distributed random variables with zero mean and unit variance (normality assumption), s_0 and s are the constant standard deviations of the two error terms (homoskedasticity assumption), and $\mathbf{\Theta}_b = (\lambda, \alpha, s_0, s)$ is a vector of unknown parameters introduced to fit the data.

A Bayesian approach was used to estimate the statistics (means, variances, and correlation coefficients) of the unknown parameters based on long-term exposure data (up to 7 years of exposure to actual environmental conditions) on 10M (#3), 16M (#5), and 19M (#6) bars from three different manufacturers. Table 1 lists the posterior statistics of $\mathbf{\Theta}_b$.

Table 1. Posterior Statistics of Unknown Parameter $\mathbf{\Theta}_b$ [Adapted from Trejo et al. (2009)]

Parameter	Mean	Standard Deviation	Correlation Coefficient			
			λ	α	s_0	s
λ	0.135	0.011	1	– 0.84	– 0.04	– 0.28
α	0.207	0.082	– 0.84	1	0.04	– 0.25
s_0	0.039	0.003	– 0.04	0.04	1	– 0.02
s	0.557	0.043	– 0.28	– 0.02	– 0.25	1

TIME-VARIANT CAPACITY OF GFRP-REINFORCED BRIDGE DECKS

Because GFRP bars have high tensile strength and exhibit brittle failure modes, the design of members with GFRP reinforcement uses a different design philosophy than a steel reinforced member. To prevent catastrophic failure of the deck, the deck is over-reinforced to ensure a concrete crushing failure rather than bar yielding. The nominal flexural strength is estimated based on strain compatibility, load equilibrium, and possible failure modes (either concrete crushing or bar rupture failure mode) (ACI 440.1R-17 2006). Bridge decks are typically designed and analyzed using a unit-wide strip deck model, rectangular cross-section.

In this paper, the constitutive model of concrete is assumed to be Todeschini's parabolic stress-strain relationship with strain ranging from maximum tensile and ultimate strain (herein 0.0035). The constitutive model for the GFRP bar is assumed to be a linear elastic stress-strain relationship with a constant MOE. The ultimate stress and strain are determined by the time-variant capacity model. To consider the degradation and failure of each individual bar, the load distribution concept is used. Each bar is considered to be a random variable and the capacity of each bar is summed to calculate the moment capacity of the section as follows:

$$f_c(\varepsilon) = \frac{1.8 f_c'\left(\varepsilon/\varepsilon_{cc}\right)}{1+\left(\varepsilon/\varepsilon_{cc}\right)^2} \tag{2}$$

where f_c' is actual compressive strength [MPa (ksi)], $f_c(\varepsilon)$ is the compressive stress at the compressive strain, ε [MPa (ksi)], ε_{cc} is $1.7\, f_c'/E_c$ and is the peak strain, E_c is the concrete MOE and is computed as (Gardoni et al. 2007):

$$\ln\left(E_c\right) = \theta_1 + \theta_2 \cdot \ln\left(f_c'\right) + \theta_3 \cdot \ln\left(w\right) + s_E \cdot e_E \tag{3}$$

where w is the unit weight of concrete, s_E is the standard deviation of the model error, e_E is a normally distributed random variable with zero mean and unit variance (normality assumption), and $\mathbf{\Theta}_E = (\theta_1, \theta_2, \theta_3, s_E)$ is a vector of unknown parameters introduced to fit the data. Table 2 lists the posterior statistics of $\mathbf{\Theta}_E$.

Table 2. Posterior Statistics of Unknown Parameter $\mathbf{\Theta}_E$ [Adapted from Gardoni et al. (2007)]

Parameter	Mean	Standard Deviation	Correlation Coefficient			
			θ_1	θ_2	θ_3	s_E
θ_1	–5.29	0.975	1	– 0.39	– 0.98	0
θ_2	0.265	0.007	– 0.39	1	– 0.42	0
θ_3	1.90	0.126	– 0.98	– 0.42	1	0
s_E	1	0	0	0	0	1

The moment capacities of a bridge deck can be estimated using the time-variant bar capacity model, the dominant failure mode, strain compatibility, and force equilibrium. The following equation can be used to determine the capacity of a deck at time *t*:

$$C_t\left(\mathbf{x},\mathbf{\Theta}\right) = \min\left[C_{CF,t}, C_{BF,t}\right] \tag{4}$$

where $C_{CF,t}$ is the nominal moment capacity of the deck when the concrete crushing failure occurs at time t, $C_{BF,t}$ is the nominal moment capacity of the deck when the GFRP bar failure occurs at time t, $\mathbf{\Theta} = (\mathbf{\Theta}_b, \mathbf{\Theta}_E)$, $\mathbf{x} = (\mathbf{x}_b, \mathbf{x}_d)$, where $\mathbf{x}_d = (f'_c, E_c, \varepsilon_{cu}, b, h, d, A_f, R_0, \sigma_{t(i)}, E_f, \varepsilon_f, n)$, A_f is the area of the GFRP reinforcement in the given section [mm^2 (in.^{2})], ε_f is the strain of the GFRP reinforcement at the concrete crushing strain in the top fiber, ε_{cu}, E_f is the MOE of the GFRP reinforcement [MPa (ksi)], b is the width of the cross section [mm (in.)], d is the distance from the extreme compression fiber to the centroid of tension reinforcement [mm (in.)], h is the depth of the section [mm (in.)], $\sigma_{t(i)}$ is the capacity at time *t* (years) of the *i*th individual GFRP bar, and *n* is the number of GFRP bars provided in the given section ($n = b/s$), where *s* is the bar spacing. The nominal moment capacity can be estimated as follows:

$$C_t = A_f E_f \varepsilon_f \left(d - c + \bar{y}\right) + \sigma e \tag{5}$$

where c is the distance measured from the top extreme fiber to the neutral axis, $\bar{y}$ is the distance from the neutral axis to the location of resultant compression force, and ε_f is the strain in the GFRP reinforcement when the concrete strain reaches crushing failure.

When the concrete crushing failure is dominant ($C_t\left(\mathbf{x},\Theta\right) = C_{CF,t}$), the strain in the GFRP bar can be determined using the following equation:

$$\varepsilon_f = 0.5\left[\varepsilon_{cu}{}^2 + \frac{4 \cdot b \cdot d}{E_f \cdot A_f} \cdot \int_0^{\varepsilon_{cu}} f_c\left(\varepsilon\right) \cdot d\varepsilon\right]^{0.5} - 0.5 \cdot \varepsilon_{cu} \le \varepsilon_{fu} \tag{6}$$

where the terms have been defined earlier. The calculated GFRP bar strain can be used to estimate the nominal moment, $C_{CF,t}$ using Eq. (5). When the bar failure is dominant

($C_t(\mathbf{x},\Theta)=C_{BF,t}$) the maximum strain in the concrete, ε_c, should be smaller than ultimate strain, ε_{cu}. To determine the concrete strain, ε_c, strain compatibility and force equilibrium conditions can be used:

$$\frac{\sum_{i=1}^{n}\sigma_{t(i)}}{n}\cdot A_f\cdot\left(\frac{\sum_{i=1}^{n}\sigma_{t(i)}}{n\cdot E_f}+\varepsilon_c\right)-b\cdot d\cdot f_c'\cdot\varepsilon_c\cdot\frac{0.9\cdot\ln\left[1+\left(\varepsilon/\varepsilon_{cc}\right)^2\right]}{\varepsilon/\varepsilon_{cc}}=0 \qquad (7)$$

Eq. (7) is only valid when the concrete strain is less than the value of ε_{cu} and the value of c is less than the value of c_b ($=\varepsilon_{cu}\cdot d/(\varepsilon_{cu}+\varepsilon_{fu})$). The nominal moment, C_{BF} can be estimated using Eq. (5) with $\varepsilon_f=\varepsilon_{fu}$.

Assessment of Deck Fragility

Fragility is defined as the conditional probability of not meeting a specified performance level for a given moment demand, D. In assessing the fragility, a limit state function $g(\cdot)$ is introduced such that the event $\{g(\cdot)\le 0\}$ denotes not meeting a specified performance level. Using the probabilistic model for the time-variant capacity of a GFRP deck described in Eq. (4), a limit state function is written as:

$$g_t(\mathbf{x},\mathbf{\Theta})=C_t(\mathbf{x},\mathbf{\Theta})-D \qquad (8)$$

The fragility at any time t is then written as:

$$F_t(D,\mathbf{\Theta})=P\left[g_t(\mathbf{x},\mathbf{\Theta})\le 0\,\middle|\,D\right] \qquad (9)$$

The uncertainty in Eq. (9) arises from the inexact nature of the model $C_t(\mathbf{x},\mathbf{\Theta})$ captured in e_0, e, and e_E, the inherent randomness (or aleatory uncertainty) in $\mathbf{x}$, and the statistical uncertainty in $\mathbf{\Theta}$. Figure 1 shows a conceptual three-dimensional plot of $F_t(D,\mathbf{\Theta})$ as a function of D and t. Following Gardoni et al. (2002), two estimates of $F_t(D,\mathbf{\Theta})$ are possible based on different treatments of the parameter uncertainties: point and predictive estimates.

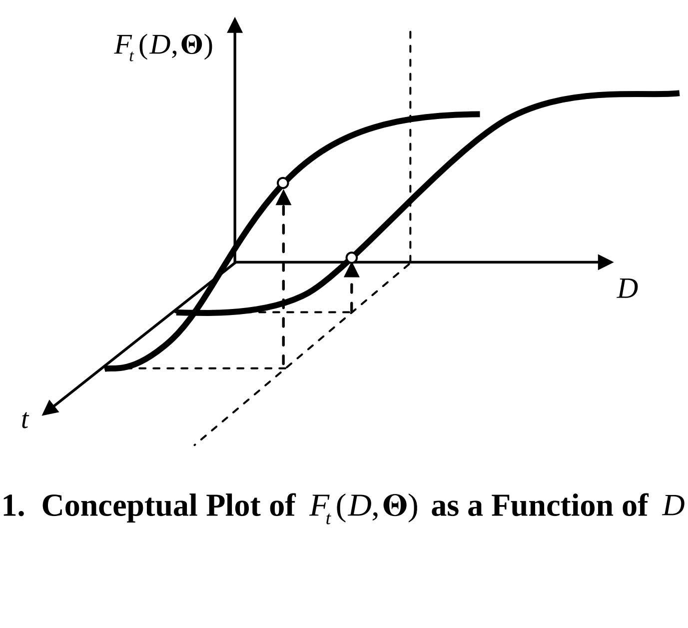

Fig. 1. Conceptual Plot of $F_t(D,\mathbf{\Theta})$ as a Function of D and t

Point Estimates

A point estimate of $F_t(D,\mathbf{\Theta})$ ignores the epistemic uncertainties in the model parameters $\mathbf{\Theta}$ and uses a point estimate $\hat{\mathbf{\Theta}}$ (e.g., the posterior mean of $\mathbf{\Theta}$) in place of $\mathbf{\Theta}$, i.e.;

$$\hat{F}_t(D) = F(D,\hat{\mathbf{\Theta}}) \tag{10}$$

Predictive Estimates

A predictive estimate is obtained as the expected value of $F_t(D,\mathbf{\Theta})$ over the posterior distribution of $\mathbf{\Theta}$, $f_{\mathbf{\Theta}}(\mathbf{\Theta})$, i.e.;

$$\tilde{F}\left(D\right) = \int_{\mathbf{\Theta}} F\left(D,\mathbf{\Theta}\right) f_{\mathbf{\Theta}}(\mathbf{\Theta})\, d\mathbf{\Theta} \tag{11}$$

where the epistemic uncertainties are incorporated into the predictive estimates of the fragility in an average sense. Eq. (11) typically needs to be solved numerically.

DECK DESIGN APPLICATION

In this section, the probability models to predict the GFRP bar and deck capacities are used to estimate the fragility curve of a typical GFRP-reinforced bridge deck designed in accordance with the AASHTO specifications (2000).

Capacity for Example of GFRP-Reinforced Bridge Deck

The GFRP reinforced bridge deck (Morristown bridge) was used to analyze the time-variant capacity reported by Benmokrane et al. (2006). The Morristown bridge is located in Morristown, Vermont, USA. This bridge is a steel girder type with five 43 m (141 ft) span length. The deck is a 230 mm (8 in.) thick concrete slab with 2.36 m (7.74 ft) girder spacing. The deck was designed according to the AASHTO specification (AASHTO 2000) and and followed the American Concrete Institute (ACI) design guideline (ACI 440.1R-01). Based on the serviceability criteria [maximum crack width = 0.5 mm (0.02 in.)], 16M (#5) GFRP reinforcing bars with 100 mm (4 in.) spacing was recommended for the bottom layer in the transverse direction. The overhang section required 19M (#6) GFRP reinforcement with 100 mm (4 in.) spacing for the top layer in the transverse direction. For constructability reasons, the final design of the bridge included both 19M (#6) GFRP reinforcement in the top and bottom layers. A detailed design procedure and drawings are provided in Benmokrane et al. (2006). In this study, only the deck section between the girders is analyzed. Table 3 presents two different design cases. Design I uses 19M (#6) GFRP reinforcement to achieve the same nominal moment in accordance with AASHTO and ACI design (Benmokrane et al. 2006). Design II uses 13M (#4) GFRP reinforcements to produce the same nominal moment as Design I.

Table 3. Design of GFRP Reinforced Deck

Design Case	Parameter	Mean	Standard Deviation	Distribution
Design I	19M (#6) R_o (mm)	9.53	0.0715	Lognormal (COV=0.75%)
	spacing (mm)	140	N.A.	Deterministic
Design II	13M (#4) R_o (mm)	6.35	0.0476	Lognormal (COV=0.75%)
	spacing (mm)	67	N.A.	Deterministic

Table 4 shows the input parameters for assessing the probability of failure for the GFRP reinforced deck. The standard deviation of the GFRP reinforcement and the concrete properties are estimated based on Nowak and Szerszen (2003) and Kulkarni (2006). The statistics of the capacities at t = 0, the elasticity values, and the diffusion coefficients of GFRP were obtained from Trejo et al. (2005, 2009, and 2010) and Gardoni et al. (2010).

Table 4. Parameters of GFRP Reinforced Deck

Materials	Properties	Parameter	Mean	Standard Deviation	Distribution
GFRP	MOE	E_f (MPa)	38,470	4355	Lognormal
	Capacity at t=0	$\mu_{\sigma 0}$ (MPa)	569	53	Lognormal
	Diffusion Coefficients	D (m^2/sec)	8.903 x 10^{-13}	3.522 x 10^{-13}	Lognormal
Deck	Compressive strength	f_c' (MPa)	30.5	2.50	Lognormal
	Crushing strain	ε_{cu} (mm/mm)	0.0035	N.A.	Deterministic
	Clear cover	c (mm)	38.1	N.A.	Deterministic
	Depth	h (mm)	228.6	N.A.	Deterministic
	Effective depth	d (mm)	$d=h–c–R_0$	N.A.	Lognormal

The flexural demand is estimated using the equivalent strip method (Article 4.6.2 in AASHTO 2007). The service limit moment, M_S, is calculated with the summation of unfactored dead load moment, unfactored live load positive moment including multiple presence factors, the dynamic load allowance factor (0.33), and the unfactored future wearing dead load moment. The as-built girder spacing of 2.36 m (7.75 ft) and the future wearing surface of 12.7 mm (0.5 in.) thickness are used for estimating the demand of 27.9 kN-m/m (6.27 kip-ft/ft). When the design moment, M_D, is considered, the demand is estimated to be 47.3 kN-m/m (10.6 kip-ft/ft).

FRAGILITY ESTIMATES

Because a typical GFRP reinforced bridge is over-reinforced to prevent catastrophic bar failure, concrete crushing failure control is desirable. However, as the degradation of GFRP bars progresses the probability of GFRP bar failure in the deck increases. GFRP reinforcement 19M (#6) in a deck tends to fail via concrete crushing failure up to approximately approximately 200 years. However, the 13M (#4) GFRP reinforcement in a deck tends to fail via concrete crushing failure after only 50 years. That is, after 50 years the bar failure governs. This estimate is based on the mean value of the GFRP and concrete properties.

As shown in Figure 2, the fragility curves of the two design examples are assessed at time, t = 0 and 75 years. As mentioned previously, the fragility curve of Design I is identical to that of Design II at time, t = 0. At time, t = 0, the probability of failure of deck is lower than 10^{-6} for $D = M_S$ and $D = M_D$ for both bar diameters. After 75 years the probability of failure increases significantly in particular when 13M (#4) bars are used. For example, at the service moment, M_S, the probability of failure of a deck with 13M (#4) bar is approximately 45% higher than that of a deck with 19M (#6) bar - 0.025 versus 0.005. At the design moment level, the probability of failure of a deck with 13M (#4) bar is four times higher at 75 years when compared to the probability of a deck with 19M (#6) bar - 0.044 versus 0.011.

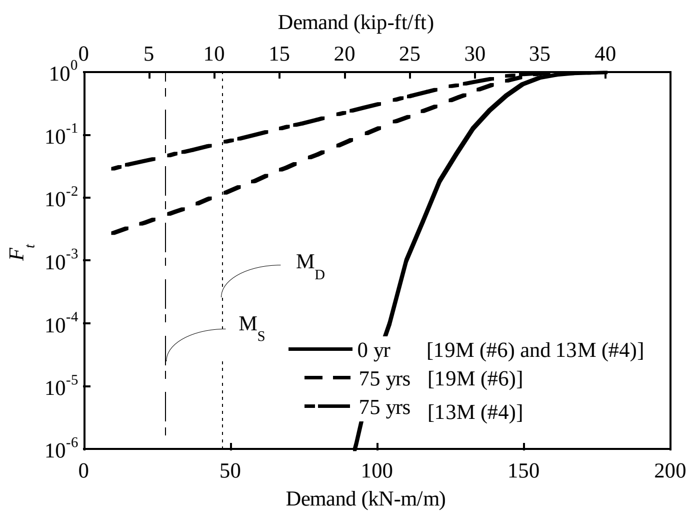

Fig. 2. Fragility Curves of Two Design Examples at *t* = 0 and 75 years

This research indicates that a bridge deck reinforced with 13M (#4) GFRP bars and 19M (#6) GFRP bars have probabilities of failure of 0.025 and 0.005. The generally accepted probability of failure for bridge structures based on the AASHTO LRFD is 0.001. Both GFRP-reinforced decks evaluated here exceed the generally accepted AASHTO probability of failure limit after 75 years of exposure. This indicates that the environmental exposure factor, C_E, may not account for the expected degradation of the GFRP bars at later ages and consideration should be given to reducing the environmental exposure factor for exterior exposure conditions. However, this research is applicable for the environmental conditions used in the research.

CONCLUSIONS

GFRP reinforcing bars have been identified as potential alternatives to steel reinforcement. ACI and AASHTO provide procedures for designing reinforced concrete structures with this type of reinforcement. Although significant research has been performed on the time-variant tensile capacity of GFRP reinforcing bars exposed to solutions, only short-term studies have been performed to assess the time-variant tensile capacity of GFRP reinforcing bars embedded in concrete. This paper uses a model for estimating the time-variant tensile capacity of GFRP reinforcing bars embedded in concrete developed by Trejo et al. (2009,

2010) and Gardoni et al. (2010). Data used to develop the model were based on shorter-term data from the literature and longer-term data obtained by Trejo et al. (2009, 2010); all data from GFRP reinforcing bars embedded in concrete. Using this time-variant model for the GFRP reinforcement, an analysis was performed to assess the time-variant capacity of two separate bridge decks reinforced with different sizes of GFRP reinforcing bars. Results from the analysis indicate that larger diameter GFRP reinforcing bars can provide lower probabilities of failure when embedded in concrete. As the GFRP diameter decreases, the probability of failure increases. The analysis also indicates that the probability of failure of the decks containing both 13M (#4) and 19M (#6) GFRP bars exhibit higher probability of failures than failure limits generally accepted by AASHTO. Reducing the environmental exposure factor, C_E, for GFRP-reinforced bridge decks (i.e., exterior exposure conditions) may be warranted.

REFERENCE

American Association of State Highway and Transportation (AASHTO) (2000), "Standard Specification for Design of Highway Bridge," *AASHTO*, Washington, D.C.

American Association of State Highway and Transportation Officials Load and Resistance Factor Design (AASHTO LRFD) (2007), "Standard Specification for Design of Highway Bridge," *AASHTO*, Washington, D.C.

American Association of State Highway and Transportation Officials Load and Resistance Factor Design (AASHTO LRFD) (2008), "Bridge Design Guide Specifications for GFRP Reinforced Concrete Decks and Deck Systems," *AASHTO*, Washington, D.C.

ACI Committee 440 (2007). "Report on Fiber-Reinforced Polymer (FRP) Reinforcement for Concrete Structures". Farmington Hills, MI., American Concrete Institute.

ACI Committee 440.1R-17 (2006), "Guide for the Design and Construction of Concrete Reinforced with FRP Bars," Farmington Hills, MI, American Concrete Institute.

Almusallam, T. H., Al-Salloum, Y. A., Alsayed, S. H., and Alhozaimy, A. M. (2002), "Tensile Strength of GFRP Bars in Concrete Beams Under Sustained Loads at Different Environments," *Second Int. Conf. on Durability of Fiber Reinforced Polymer (FRP) Compos. for Constr.*, Sherbooke, Quebec, Canada, May 29-31, 2002, 523-533.

Benmokrane, B., El-Salakawy, E.F., El-Ragaby, A., and Lackey, T. (2006), "Design and Testing of Concrete Bridge Deck Slabs Reinforced with Glass FRP Bars," *ASCE J. of Bridge Engrg.*, 11(2), 217-229.

Debaiky, A. S., Nkurunziza, G., Benmokrane, B., and Cousin, P. (2006), "Residual tensile properties of GFRP reinforcing bars after loading in severe environments," *J. of Compos. for Constr.*, 10(5), 370-380.

Gardoni, P., Der Kiureghian A., Mosalam K.M., (2002), "Probabilistic capacity models and fragility estimates for RC columns based on experimental observations," *ASCE J. of Engrg.* Mechanics, 128 (10), 1024-1038.

Gardoni, P., Nemati, K.M., and Noguchi, T., (2007), "Bayesian statistical framework to construct probabilistic models for the elastic modulus of concrete," *ASCE J. of Mater. in Civil Engrg.*, 19(10), 898-905.

Gardoni, P., Trejo, D., Kim, J. J. (2010), "Time-variant capacity model for GFRP bars embedded in concrete" *ASCE Journal of Composites for Construction* (submitted).

Giernacky, R. G., Bakis, C. E., Mostoller, J. D., Boothby, T. E., and Mukherjee, A. (2002), "Evaluation of Concrete Beams Reinforced with Internal GFRP Bars: A Long-Term Durability Study," *Second Int. Conf. on Durability of Fiber Reinforced Polymer (FRP) Compos. for Constr. (CDCC 02)*, Montreal, Quebec, Canada, May, 39-45.

Katsuki, F., and Uomoto, T. (1995), "Prediction of Deterioration of FRP Rods due to Alkali Attack," *Proceedings of the Second International RILEM Symposium (FRPRCS-2)*, Non-Metallic (FRP) Reinforcement for Conc. Struct., L. Taerwe, ed., E&FN Spon, London, 83-89.

Kulkarni, S. (2006), "Calibration of flexural design of concrete members reinforced with FRP bars," M.S. Thesis, Louisiana State University, May 2006.

Micelli, F., and Nanni, A. (2004), "Durability of FRP rods for concrete structures," Construction *and Build. Mater*., 18(7), 491-503.

Micelli, F., Nanni, A., and Tegola, A. L. (2001), "Effects of Conditioning Environment on GFRP Bars," *22nd SAMPE Europe Int. Conf.* CNIT, Paris, 1-13.

Mufti, A., Banthia, N., Benmokrane, B., Boulfiza, M., and Newhook, J. (2007a), "Durability of GFRP composite rods," *Conc. Int.*, American Concrete Institute, 37-42.

Mufti, A. A., Onofrei, M., Benmokrane, B., Banthia, N., Boulfiza, M., Newhook, J. P., Bakht, B., Tadros, G. S., and Brett, P. (2007b), "Field study of glass-fibre-reinforced polymer durability in concrete," *Can. J. of Civil Engrg*, 34(3), 355-366.

Mukherjee, A. and Arwikar, S. J. (2005), "Performance of glass fiber-reinforced polymer reinforcing bars in tropical environments-part I: Structural scale tests," *ACI Struct. J.* 102(5), 745-753.

Nowak, A.S. and Szerszen, M.M. (2003), "Calibration of Design Code, for Buildings (ACI318): Part 1- Statistical Models for Resistance," *ACI Struct J*., Vol. 100, No. 3, 377-382.

Robert, M., Cousin, P., and Benmokrane, B. (2009), "Durability of GFRP Reinforcing Bars Embedded in Moist Concrete," *Journal of Composites and Constructions*, 66-73.

Svecova, D., Rizkalla, S., Vogel, H., and Jawara, A. (2002), "Durability of GFRP in Low-Heat High Performance Concrete," *2nd International Conf. on Durability of Fiber Reinforced Polymer (FRP) Compos. for Constr.*, Sherbrook, Quebec, Canada, May 29-31, 75-86.

Tannous, F. E., and Saadatmanesh, H. (1999), "Durability of AR glass fiber reinforced plastic bars," *Journal of Compos. for Constr.*, 3(1), 12-19.

Todeschini, C. E., Bianchini, A. C., Kesler, C. E. (1964), "Behavior of Concrete Columns Reinforced with High Strength Steels," *ACI J., Proceedings*. 61 (6), 701-716.

Trejo, D., Aguiniga, F., Yuan, R., James, R. W., and Keating, P. B. (2005), Characterization of Design Parameters for Fiber Reinforced Polymer Composite Reinforced Concrete Systems, Texas Transportation Institute Research Report 9-1520-3.

Trejo, D., Gardoni, P., Kim, J. J., Zidek, J. (2009a), "Long-term performance of GFRP reinforcement: Technical Report," Texas Transportation Institute Research, *Report 0-6069-1*, 134

Trejo, D., Gardoni, P., Kim, J. J. (2010), "Long-term performance of glass fiber-reinforced polymer reinforcement," ACI Material Journal (submitted).